ACS APPLIED MATERIALS & INTERFACES

Research Article

www.acsami.org

Gelatin Microgel Incorporated Poly(ethylene glycol)-Based Bioadhesive with Enhanced Adhesive Property and Bioactivity

Yuting Li, Hao Meng, Yuan Liu, Ameya Narkar, and Bruce P. Lee*

Department of Biomedical Engineering, Michigan Technological University, Houghton, Michigan 49931, United States

Supporting Information

ABSTRACT: Up to 7.5 wt % of chemically cross-linked gelatin microgel was incorporated into dopamine-modified poly(ethylene glycol) (PEGDM) adhesive to simultaneously improve the material property and bioactivity of the PEG-based bioadhesive. Incorporation of gelatin microgel reduced cure time while it increased the elastic modulus and cross-linking density of the adhesive network. Most notably, the loss modulus values for microgel-containing adhesive were an order of magnitude higher when compared to microgel-free control. This drastic increase in the viscous dissipation ability of the adhesive is attributed to the introduction of reversible physical bonds into the adhesive network with the incorporation of the gelatin microgel. Additionally, incorporation of the microgel increased the adhesive properties of PEGDM by 1.5- to 2-fold. From in vitro cell culture studies, the composite adhesive is noncytotoxic and the incorporation of microgels provided binding site for promoting fibroblast attachment and viability. The subcutaneous implantation study indicated that the microgel-containing PEGDM adhesive is biocompatible and the incorporated microgels provided pockets for rapid cellular infiltration. Gelatin microgel incorporation was demonstrated to be a facile method to simultaneously enhance the adhesive property and the bioactivity of PEG-based adhesive.

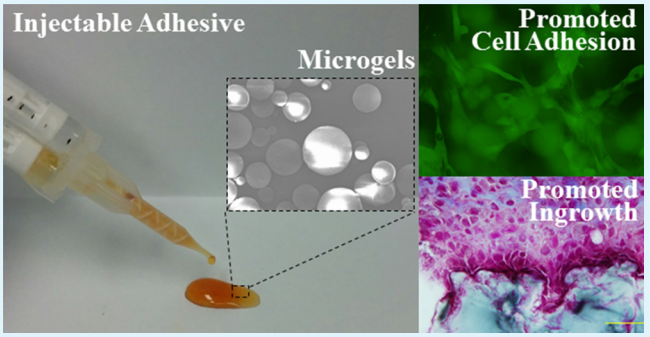

KEYWORDS: *bioadhesive, poly(ethylene glycol), gelatin microgel, dopamine, bioactivity*

INTRODUCTION

Poly(ethylene glycol) (PEG) is a biocompatible and non-immunogenic polymer commonly used in designing various biomaterials.[1,2] Numerous PEG-based sealants and bioadhesives are commercially available (e.g., Coseal, Baxter Healthcare Corporation and DuraSeal, Integra LifeSciences). However, PEG is bioinert and lacks the ability to promote cellular attachment and infiltration needed for rapid tissue repair and regeneration.[3] To improve the bioactivity of PEG-based biomaterials, various short peptide sequences and bioligands (i.e., Arg-Gly-Asp,[4] Arg-Glu-Asp-Val,[5] and cysteine-containing peptides[6]) have been tethered to PEG to promote cell adhesion and proliferation. However, functionalizing PEG with bioactive peptide sequences requires multistep chemical synthetic approach, which is associated with low yield and high cost. Most importantly, peptide functionalization does not increase the mechanical properties of these PEG-based materials.

To simultaneously improve the mechanical and adhesive properties and the bioactivity of PEG-based adhesive, gelatin microgels were incorporated into an injectable adhesive formulation. Gelatin is a soluble protein hydrolyzed from collagen, which is the main structural component of extracellular matrix and supports cell adhesion, migration, and proliferation.[7−9] Gelatin is nontoxic and biodegradable in vivo[10] and exhibits lower antigenicity when compared to collagen.[11,12] However, gelatin is insoluble at room temperature due to extensive physical bonds and requires heating beyond the physiological temperature to achieve dissolution. This heating requirement makes it impractical for formulating gelatin polymer directly into an in situ curable bioadhesive. Direct injection of gelatin microgels as a suspension has been previously reported for drug delivery[13] and tissue engineering[14] applications. The ability to incorporate gelatin microgels into an injectable PEG-based adhesive is examined here.

Branched PEG end-functionalized with dopamine (PEGDM) was used as the PEG-based adhesive in this study. Dopamine mimics the catecholic amino acid, 3,4-dihydroxyphenylalanine (DOPA), found in the mussel adhesive protein, which is responsible for rapid curing and interfacial binding of the protein in a saline and wet environment.[15] The catechol moiety has the capability to undergo various catechol−catechol or catechol−surface cross-linking (Scheme 1). Catechol groups can be oxidized into highly reactive quinones, which reacts with other catechol residues to achieve rapid curing of the adhesive.[16,17] Quinones can also chemically cross-link with nucleophilic groups including lysyl, cystainyl, and histidyl groups found in natural tissues, resulting in the formation of interfacial covalent bonds.[18,19] Inert, synthetic polymers

Received: February 1, 2016
Accepted: April 25, 2016
Published: April 25, 2016

DOI: 10.1021/acsami.6b01364
ACS Appl. Mater. Interfaces 2016, 8, 11980−11989

Scheme 1. Schematic Illustration of the Reactions between PEGDM and Gelatin Microgel or Tissue Substrates[a]

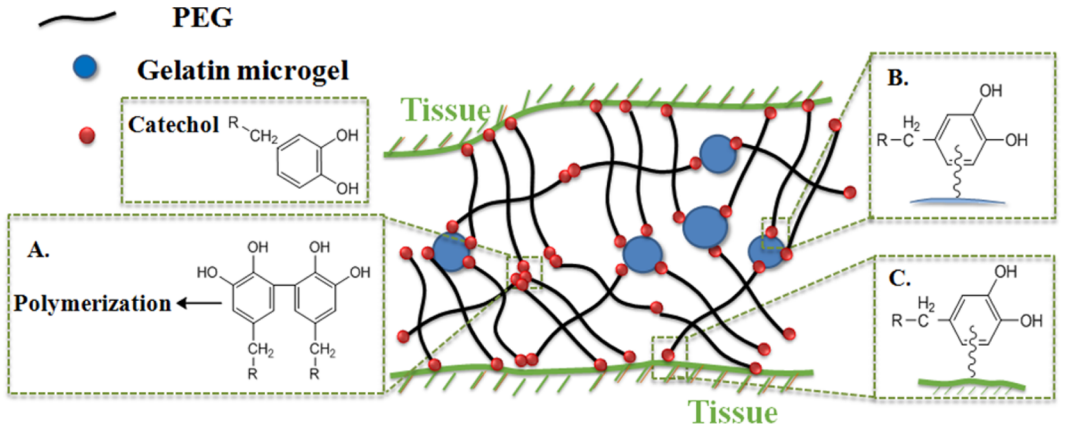

[a]Catechol groups are oxidized to form reactive quinone, which can result in cohesive cross-linking and curing of the adhesive (A), and interfacial cross-linking with nucleophilic functional groups (i.e., $-NH_2$, −SH) found on either the gelatin microgels (B) or tissue surface (C).

modified with DOPA and other catechol derivatives (i.e., dopamine) have demonstrated strong, water-resistant adhesive properties to various biological, metallic, and polymeric substrates.[15,20,21]

In this work, we combined PEGDM with up to 7.5 wt % of chemically cross-linked gelatin microgels to prepare a novel composite bioadhesive (Scheme 1). The effects of microgel incorporation on the mechanical and adhesive properties of the adhesive were determined. Additionally, the effect of the encapsulated microgels on the cytotoxicity and cell attachment to the adhesive surface was examined in culture. Finally, the biocompatibility and the ability for the composite adhesive to promote cellular infiltration were examined through subcutaneous implantation in rat.

EXPERIMENTAL SECTION

Materials. Gelatin powder (type A, 300 Bloom, from porcine skin) was purchased from Electron Microscopy Sciences. Sodium periodate ($NaIO_4$, ACS reagent, >99.8%), pyridine (ACS reagent, >99.0%), 1-ethyl-3-[3-dimethylaminopropyl]carbodiimide hydrochloride (EDC), *N*-hydroxysuccinimide (NHS), Masson's trichrome stain kit, bouin solution, Weiger's iron hematoxylin solution, TWEEN 80, and glutaric anhydride were purchased from Sigma-Aldrich. Dulbecco's modified Eagle medium (DMEM) was obtained from Corning Cellgro. Fetal bovine serum (FBS) was purchased from Thermo Scientific. Sodium pyruvate (100 mM), MEM nonessential amino acid (100×), and 4-(2-hydroxyethyl)-1-piperazineethanesulfonic acid (HEPES) buffer solution (1 M) were purchased from Life Technologies. 8-arm poly(ethylene glycol) (20K) was purchased from JenKem Technology. Dopamine hydrochloride was purchased from Acros Organics. *O*-(Benzotriazol-l-yl)-*N*,*N*,*N*′,*N*′-tetramethyluronium hexafluorophosphate (HBTU) and 1-hydroxybenzotriazole monohydrate (HOBt) were purchased from Chem-Impex International. Phosphate buffer saline (PBS) and *N*,*N*-dimethylformamide (DMF) were purchased from Fisher Scientific. Chloroform was purchased from J. T. Baker. 3-(4,5-Dimethylthiazol-2-yl)-2,5-diphenyltetrazolium bromide (MTT) 98% was purchased from Alfa Aesar. 4′,6-Diamidino-2-phenylindole (DAPI) was purchased from Invitrogen. Anti-S100A4 antibody (ab27957), goat anti-rabbit IgG H&L (Alexa Fluor 488; ab150077), anti-CD11b antibody (ab8879), and goat anti-mouse IgG (Alexa Fluor 488; ab150113) were purchased from Abcam. Anti-CD163 antibody (sc-58965) and goat anti-mouse IgG (sc-2781) were purchased from Santa Cruz Biotechnology. Rat dermal fibroblast was isolated from rat dermal tissue and identified with anti-S100A4 antibody and goat anti-rabbit IgG H&L (Alexa Fluor 488).[22] A 12-well cell suspension culture plate was purchased from VWR International. Mechanical sieves were purchased from ATM Corporation. Dialysis tubing was purchased from Spectrum Labs (MWCO 3500).

Synthesis of Dopamine-Modified PEG (PEGDM). Biodegradable PEGDM was synthesized in two steps. In the first step, glutaric acid was chemically linked to the terminal end-group of PEG (PEGGlu) through ester bond formation. In the second step, the acid end-group of PEGGlu was reacted with the amine group of dopamine forming PEGDM through the formation of amide bond. To synthesize PEGGlu, 32 g of 8-arm PEG and 7.30 g of glutaric anhydride were dissolved with 300 mL of chloroform, which was further combined with 5.16 mL of pyridine. The polymer solution was refluxed under nitrogen for 24 h, and then the solvent was removed. The crude polymer was dissolved in deionized water (DI) at a concentration of 25 mg/mL and dialyzed for 48 h using a dialysate with a pH adjusted to around 3. After lyophilization, 30 g of PEGGlu was obtained with a coupling efficiency of 81% based on ^{1}H NMR. ^{1}H NMR (400 MHz, D_2O) δ 3.75−3.39 (m, PEG), 2.37 (t, 2H, $-C(=O)-(CH_2)_2-CH_2-C(=O)-$), 2.32 (t, 2H, $-C(=O)-(CH_2)_2-CH_2-C(=O)-$), 1.79 (t, 2H, $-C(=O)-(CH_2)_2-CH_2-C(=O)-$) (Figure S1 in Supporting Information).

In the second step, 30 g of PEGGlu, 5.45 g of dopamine HCl, 3.70 g of HOBt, and 9.16 g of HBTU were combined with 120 mL of chloroform, 60 mL of DMF, and 4.0 mL of triethylamine. After reacting for 3 h, the solution was rotary evaporated and dried in a vacuum desiccator. The crude polymer was dissolved in DI water at a concentration of 22 mg/mL and dialyzed for 48 h using a dialysate with a pH adjusted to around 3. After lyophilization, 28 g of PEGDM was obtained with a coupling efficiency of 80% based on ^{1}H NMR. ^{1}H NMR (400 MHz, D_2O) δ 6.71 (d, 1H, $-C_6H_2H(OH)_2$), 6.64 (d, 1H, $-C_6H_2H(OH)_2$), 6.56 (d, 1H, $-C_6H_2H(OH)_2$), 3.74−3.38 (m, PEG), 2.12 (t, 2H, $-C(=O)-(CH_2)_2-CH_2-C(=O)-$), 2.07 (t, 2H, $-C(=O)-(CH_2)_2-CH_2-C(=O)-$), 1.67 (t, 2H, $-C(=O)-(CH_2)_2-CH_2-C(=O)-$) (Figure S2).

Preparation of Gelatin Microgel. Physically cross-linked gelatin microgel was prepared with water-in-oil emulsification method. An amount of 2 g of gelatin powder was dissolved in 20 mL of DI water and stirred with magnetic stir bar for 10 min in a heated water bath (50−55 °C). The gelatin solution was then added dropwise into 200 mL of preheated olive oil (50−55 °C), which was stirred at 1000 rpm using an overhead mechanical stirrer for 1 h to form an emulsion. The temperature of the emulsion was lowered and kept at room temperature for 30 min with continued stirring. The emulsion was then placed in an ice−water bath for an additional 30 min with continued stirring to further solidify the microgels. An amount of 100 mL of precooled acetone (4 °C) was added into the emulsion mixture to precipitate the microgel, and the mixture was further stirred for 30 min in the ice−water bath. The microgel was separated from olive oil and acetone through vacuum filtration and further washed twice with

DOI: 10.1021/acsami.6b01364
ACS Appl. Mater. Interfaces 2016, 8, 11980−11989

60 mL of precooled acetone. The size and size distribution of the microgel were controlled by filtering the microgel through a mechanical sieve (pore sizes of 53−75 μm). The yield of the physically cross-linked microgel was 0.72 g.

In order to chemically cross-link the microgel, 0.5 g of the physically cross-linked microgel was suspended in 30 mL of PBS (pH = 5.7, 0.5% TWEEN 80). 0.134 g of EDC and 0.02 g of NHS were added to the suspension, and the reaction mixture was kept at 4 °C for 24 h. After that, the microgel was washed twice with 60 mL of precooled (4 °C) acetone and collected through vacuum filtration. The yield of the cross-linked microgel was 0.43 g. The morphology of gelatin microgel was characterized with scanning electron microscope (SEM, Jeol JSM) (Figure S3).

Preparation and Characterization of Gelatin Microgel Incorporated PEGDM Adhesive. Gelatin microgel was suspended in the polymer precursor solution containing 30 wt % PEGDM dissolved in 10 mM PBS (pH 7.4) with a microgel content of 0−15 wt %. The composite adhesive was prepared by mixing equal volumes of PEGDM/microgel mixture and $NaIO_4$ solution (11.7 mg/mL in DI water). The molar ratio of $NaIO_4$ and dopamine was kept at 0.5, and the final concentrations of PEGDM and gelatin microgel were 15 wt % and 0−7.5 wt %, respectively. The cure time was determined when the mixture stopped to flow in a tilt vial.[17,23] The adhesive was allowed to cure for an additional 12 h prior to further testing. To determine the equilibrium water content (EWC), disk-shaped adhesive with a diameter of 10 mm and thickness of 1 mm (n = 4) was equilibrated in PBS (pH 7.4) at room temperature overnight and dried in vacuum for 2 days. The mass of swollen (M_s) and mass of dried (M_d) adhesive were determined to calculate EWC using the following equation:

$$\text{EWC},\% = \frac{M_s - M_d}{M_s} \times 100 \quad (1)$$

The chemical composition of the vacuum-dried adhesive was verified using Fourier transform infrared (FTIR) spectroscopy (PerkinElmer Spectrum One spectrometer).

Uniaxial Compression Testing. Adhesives (n = 6) were compressed at a rate of 0.03 mm/s until the sample fractured using a Bose ElectroForce mechanical testing machine. The dimensions of each sample (thickness of ∼3 mm and diameter of ∼7 mm) were measured individually with a digital caliper before testing. The stress was calculated by dividing the measured load by the surface area of the sample. The strain was obtained by dividing the place changes of compression plate by the original thickness of the sample. The failure stress and failure strain were determined when the first fracture occurred. Toughness was determined by the integration of the area under the stress−strain curve. The elastic modulus was determined based on the slope of the stress−strain curve at a strain between 0.05 and 0.12.

Oscillatory Rheometry. The storage (G') and loss (G'') moduli of the cured adhesive were determined using a rheometer (HR-2, TA Instruments, New Castle, DE) tested at a frequency range of 0.1−100 Hz and a stain of 0.1%. Adhesive disks (diameter of 8 mm, thickness of 1mm, n = 3) were tested using parallel plates at a gap distance that was set at 85% that of the individual adhesive thickness, as measured by a digital vernier caliper. To study the curing behavior of PEGDM adhesive, 100 μL of 300 mg/mL PEGDM adhesive precursor solution (containing either 0 or 15 wt % gelatin microgel) and 100 μL of 11.7 mg/mL $NaIO_4$ ($NaIO_4$/dopamine = 0.5) was mixed directly on the bottom fixture of the rheometer. A cone fixture (angle of 2° and diameter of 20 mm) was immediately brought down to the bottom fixture with a gap of 200 μm, and both G' and G'' values were determined at a frequency of 1 Hz and a stain of 0.1% for 10 min.

Lap Shear Adhesion Testing. Lap shear adhesion testing was performed according to the American Society for Testing and Materials (ASTM) standard F2255-05. 60 μL of the polymer precursor containing PEGDM and microgel and 60 μL of $NaIO_4$ solution were added onto one end of a piece of bovine pericardium (2.5 cm × 2.5 cm). The adhesive joint was formed by placing the second piece of pericardium tissue over the first with a 1 cm overlap. The adhesive joint was compressed with a 100 g weight for 10 min and further incubated in PBS (pH 7.4) at 37 °C overnight. The overlapped area of each adhesive joint was measured by determining its length and width using a digital caliper. The samples were pulled at a rate of 5 mm/min (8872 Instron, Norwood, MA) until the adhesive joint was completely separated, and the maximum load and displacement were recorded. The lap shear strength was calculated by dividing the max load from the initial overlapped area of the adhesive joint.[24]

In Vitro Degradation. Disk shaped adhesive (thickness of 1 mm, diameter of 8 mm, n = 3) were incubated in 2 mL of PBS (pH 7.4) at 37 °C. The PBS solution was changed every 7 days. At a given time point, samples were dried in a vacuum desiccator and weighed to determine the residual dry mass of the sample (M_t) at time t. The percent residual mass of adhesives was determined by

$$\text{residual dry mass},\% = \frac{M_t}{M_0} \times 100 \quad (2)$$

where M_0 is the average dry mass of three samples that did not undergo degradation.[25]

Cell Viability Assessment. Quantitative MTT cytotoxicity assay was conducted according to the ISO 10993-5 guideline. L929 mouse fibroblast was cultured in culture medium containing 10% FBS and 10 units/mL penicillin−streptomycin in DMEM at 37 °C. Adhesive extract was obtained by incubating the adhesive disks in the culture medium for 24 h, and the adhesive extract was sterilized using 0.22 μm sterile filters.[25] Meanwhile, cells were seeded into 96-well culture plate at the density of 1×10^4 cell/well. To each well was then added 100 μL of culture medium, and the samples were incubated for 24 h to obtain a confluent monolayer of cells. After that, the cell culture medium was replaced with 100 μL of adhesive extract and the cells were further incubated for 24 h. The adhesive extract was then replaced by 50 μL of MTT solution (1 mg/mL in PBS), and the cells were further incubated for another 2 h. Finally, all the solution was removed and replaced with 100 μL of DMSO. The absorbance was measured at 570 nm with a Synergy HT multimode microplate reader (BioTek, USA). The relative cell viability was calculated with

$$\text{relative cell viability},\% = \frac{A_{\text{adhesive}}}{A_{\text{control}}} \times 100 \quad (3)$$

where A_{adhesive} is the absorbance for cells cultured in the adhesive extract and A_{control} is the absorbance for cells cultured in cell culture medium. For each adhesive formulation, three independent cultures were prepared and cytotoxicity test was repeated three times. Samples were considered noncytotoxic when they had a relative cell viability higher than 70%.[25]

Cell Attachment Assay. Disk-shaped adhesives (thickness of 0.5mm, diameter of 10mm) were sterilized with 70% ethanol for 45 min and balanced with PBS three times, each time lasting 30 min.[25] Rat dermal fibroblasts (3.2×10^4 cells/cm^2) were seeded onto the surface of adhesive in a 12-well cell suspension culture plate. The cells were allowed to attach on the surface of adhesive for 30 min in an incubator and subsequently cultured for another 72 h at 37 °C. The attached cells were stained with DAPI (diluted in PBS at 1:1000 ratio) for 20 min, imaged using an Olympus BX51 microscope, and analyzed using ImageJ software to determine the cell density. The live/dead assay was performed by incubating the adhered cell in calcine/ethidium bromide solution (diluted in PBS at 1:1000 ratio) for 3 min and imaged using a microscope.[26]

Subcutaneous Implantation. Healthy, weight matched Sprague Dawley rats were provided by Michigan Technological University animal care facility. The subcutaneous implantation was performed following the protocol approved by Michigan Technological University Institutional Animal Care and Use Committee. Disk-shaped adhesives containing 0 and 7.5 wt % gelatin microgel (diameter of 10 mm and thickness of 1.5 mm, n = 4) were subcutaneously implanted into rats. Four bilateral pouches were created using sterile surgical scissors on the back of rats, and samples were then implanted into these pouches. Wounds were closed with surgical staples. After 2 and 6 weeks of recovery, the animals were sacrificed. Samples and the

DOI: 10.1021/acsami.6b01364
ACS Appl. Mater. Interfaces 2016, 8, 11980−11989

surrounding tissues were collected and flash frozen in Polyfreeze. Samples were sectioned into 10 μm thick sections and stained with Masson's trichrome staining to evaluate the morphology and collagen formation. Fibroblast marker (S100A4), macrophage marker (CD11b), and M2 macrophage marker (CD163) were used for immunohistochemistry staining to analyze the inflammatory response and wound healing process. Cell density was measured in 100 × 50 μm^2 area at tissue-adhesive interface. Cell infiltration layer was measured from the tissue-adhesive interface to the surrounding native tissue.[25] Collagen layer was the area closed to the implant interface (blue color in Masson's trichrome staining). All these parameters were measured using ImageJ software.

Statistical Analysis. Statistical analysis was performed using SigmaPlot software. Student t test and one-way analysis of variance (ANOVA) were used to compare the mean values of two groups and multiple groups, respectively. A statistical difference was determined when p-value was less than 0.05.

RESULTS AND DISCUSSION

Preparation and Characterization of the Composite Adhesive. Gelatin microgel was synthesized via water-in-oil emulsification method and further chemically cross-linked through the formation of amide bonds using EDC/NHS carbodiimide chemistry. From SEM image (Figure S3), the harvested microgels appeared as round spheres with an average diameter of 53.6 ± 14.2 μm. Chemical cross-linking of the microgel improves the thermal and mechanical stability of gelatin microgel[27,28] and enables the microgels to be suspended in solution and formulated into a in situ curable PEGDM adhesive.

The cure time of the PEGDM adhesive decreased with increasing weight percentage of gelatin microgel (Figure 1).

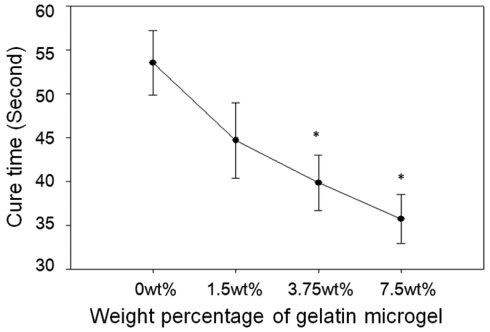

Figure 1. Cure time of PEGDM adhesive formulated with different amount of gelatin microgel. The cure time was determined when the mixture ceased to flow in a tilted vial: (*) $p < 0.05$ when compared with adhesive containing 0 wt % microgel. Error bars indicate the standard deviation, and $n = 5$.

The average cure time of microgel-free control was 54 s, and the cure time decreased gradually with increasing weight percentage of gelatin microgel, with the formulation containing 7.5 wt % microgel exhibiting the shortest gelation time (37 s). PEGDM adhesive cures through the polymerization of catechol groups in the dopamine structure (Scheme 1A) with the introduction of the chemical oxidant ($NaIO_4$).[17,24] Additionally, the quinone moiety, which is the oxidized form of the catechol group, can form covalent bond with nucleophilic groups (i.e., $-NH_2$, $-SH$) found on the gelatin microgel surface (Scheme 1B).[18] As such, the number of cohesive chemical cross-links needed for network formation was reduced with increasing microgel content and resulted in a reduced cure time.

7.5 wt % microgel was the highest amount of microgel we could incorporate into PEGDM as the precursor solution containing higher microgel content (i.e., 10 wt %) was too viscous to formulate into an injectable bioadhesive. For comparison purposes, we also attempted to incorporate gelatin polymers into PEGDM adhesive by directly blending it into the adhesive precursor solution. However, at the concentrations that were tested in this study, gelatin was not soluble in the precursor solution at room temperature. In order to dissolve gelatin, the temperature of the precursor solution needed to be increased to above 50 °C. However, the mixture solidified upon cooling as a result of physical bond formation within the gelatin polymer chains. This temperature dependent curing of gelatin made it not possible to create an in situ curable adhesive through direct blending of gelatin polymer.

FTIR spectra confirmed the incorporation of gelatin microgel into PEGDM adhesive (Figure 2). PEGDM exhibited peaks for

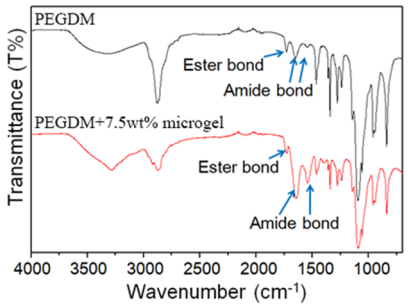

Figure 2. FTIR spectra of PEGDM adhesive (top) and the adhesive containing 7.5 wt % gelatin microgel (bottom).

ether bonds (1000−1150 cm^{-1}) of PEG, phenol (3200−3500 cm^{-1}), and aromatic (1400−1500 cm^{-1}) characteristics of catechol, and features of ester (1731 cm^{-1}) and amide (1568 and 1640 cm^{-1}) linkages used to couple glutaric acid and dopamine, respectively, to PEG. The intensity of amide bond peaks increased with the incorporation of gelatin microgel, while the intensity of ester bond remained unchanged. The increase in amide bond intensity is associated with an increase of protein content in the PEGDM adhesive.

The equilibrium water content (EWC) of PEGDM adhesive decreased with increasing gelatin microgel content (Figure 3). The EWC value for microgel-free adhesive was measured to be 90 ± 0.40%, which gradually decreased to a value of 87 ± 0.50% for an adhesive containing 7.5 wt % microgel. EWC is inversely proportional to the cross-link density of the adhesive network.[29] The incorporation of microgel increased the overall polymer concentration within the adhesive formulation and resulted in the increased cross-linking density of adhesives with increasing microgel content. Due to the hydrophilic nature of PEG, PEG-based bioadhesive is associated with excessive swelling, which could lead to severe complications such as nerve compression.[30,31] EWC data presented here indicated that microgel incorporation can be used to control the swelling of PEGDM adhesive.

Compression Testing. The results of unconfined, uniaxial compression test revealed that the incorporation of gelatin microgel increased the elastic modulus of PEGDM adhesive (Table 1). The increase in the measured modulus corresponded with increased cross-linking density of PEGDM as a result of increasing microgel content, which corroborated with the EWC results. However, incorporation of microgel did not

DOI: 10.1021/acsami.6b01364
ACS Appl. Mater. Interfaces 2016, 8, 11980−11989

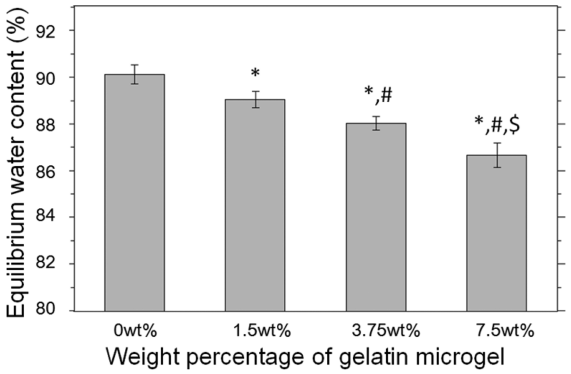

Figure 3. Equilibrium water content of PEGDM containing different weight percent of gelatin microgel: (∗) $p < 0.05$ when compared with adhesive containing 0 wt % microgel; (#) $p < 0.05$ when compared with adhesive containing 1.5 wt % microgel; ($) $p < 0.05$ when compared with adhesive containing 3.75 wt % microgel. Error bars indicate the standard deviation, and $n = 4$.

alter other parameters such as failure stress, failure strain, and toughness. The increase in the measured stiffness was achieved without compromising the compliance of the adhesive.

Oscillatory Rheometry. The viscoelastic property of adhesive was determined using an oscillatory rheometer (Figure 4). For all the formulations, the storage modulus (G') values were significantly higher than the loss modulus (G'') values, indicating that the adhesive was covalently cross-linked. G' of microgel-free PEGDM was independent of frequency at a frequency lower than 25 Hz, indicating that the sample behaved more elastically.[23] On the other hand, there was a slight increase in G' values with increasing frequency for microgel incorporated samples, and this frequency dependence increased with increasing microgel content. This result indicated that the presence of reversible physical bonds within the adhesive network is a result of gelatin microgel incorporation.[32,33] G' values increased sharply for all the samples tested at elevated frequencies (>25 Hz). This stiffening phenomenon is associated with polymer chains not having sufficient time to relax within the short time scale of the imposed mechanical deformation at elevated frequencies.[34,35]

Increased gelatin microgel content increased the measure G' values. This result is in agreement with the measured elastic modulus from compression testing, where the incorporation of microgel increased the stiffness and cross-linking density of the adhesive network. Similarly, G'' values also increased with the increasing microgel content. Most noticeably, the adhesive containing 7.5 wt % microgel exhibited G'' value that was over an order of magnitude higher than those of formulations containing 0 and 1.5 wt % microgel. The elevated G'' is associated with an increased viscous dissipation ability of

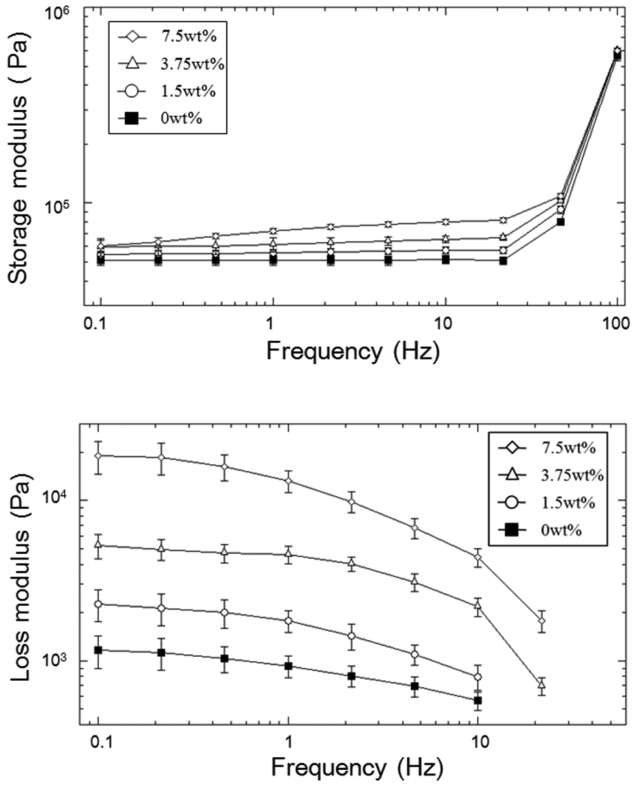

Figure 4. Storage (top) and loss (bottom) modulus of PEGDM adhesive containing different weight percentage of gelatin microgel. Error bars indicate the standard deviation, and $n = 3$.

adhesive.[32,36] Molecular chains of gelatin undergo a coil-to-helix conformational transition to form physically cross-linked networks at a lower temperature (<35 °C), and during the process gelatin molecules recover the triple helix structure of collagen.[37,38] This reversible, physical interaction is preserved within the gelatin microgel as indicated by the elevated G'' values. The presence of sacrificial bond within the adhesive network is potentially important for the dissipation of fracture energy during mechanical loading.

To study the curing behavior of the adhesive, the precursor solutions were mixed directly on the oscillatory rheometer fixture and the changes in the viscoelastic behavior of the adhesive were tracked over time. Regardless of the sample formulation, G' values were greater than those of G'' at the first measurable time point, indicating the adhesive was already chemically cross-linked (Figure 5). Due to the fast curing behavior of the PEGDM adhesive, we were unable to capture the crossover point between G' and G'' as reported by other investigators.[39] Both moduli continued to increase over time, indicating that the catechol continues to undergo chemical

Table 1. Compression Testing Results Adhesive Containing Different Amounts of Gelatin Microgel[a]

	microgel content			
	0 wt %	1.5 wt %	3.75 wt %	7.5 wt %
failure stress (kPa)	410 ± 50	460 ± 38	450 ± 36	420 ± 28
failure strain	0.64 ± 0.030	0.62 ± 0.020	0.60 ± 0.010	0.57 ± 0.030
elastic modulus (kPa)	150 ± 10	160 ± 5.1	180 ± 15*	200 ± 11*,#
toughness (kJ/m^3)	180 ± 12	200 ± 8.2	190 ± 18	200 ± 38

[a]Symbols indicate the following: (∗) $p < 0.05$ when compared with adhesive containing 0 wt % microgel. (#) $p < 0.05$ when compared to adhesives containing 1.5 and 3.75 wt % microgels.

DOI: 10.1021/acsami.6b01364
ACS Appl. Mater. Interfaces 2016, 8, 11980−11989

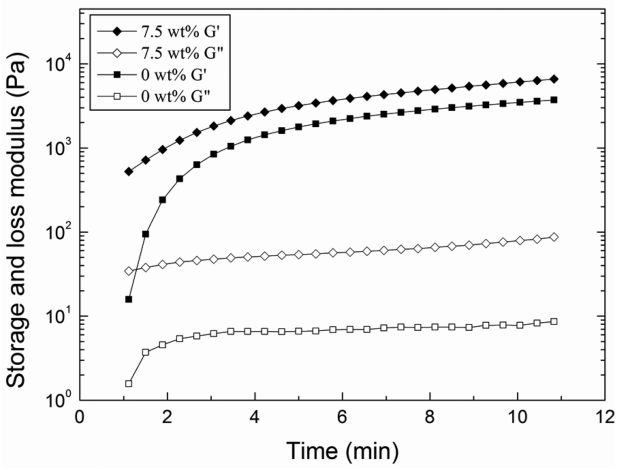

Figure 5. Storage (G', filled symbols) and loss (G'', empty symbols) moduli of PEGDM adhesive containing 0 (■, □) and 7.5 (◆, ◇) wt % gelatin microgel as a function of time after mixing the precursor solutions.

cross-linking even after the adhesive had already solidified. Catechol has been previously determined to form oligomers of up to 6 residues over several hours.[17] Even during these early time points, measured G'' values were an order of magnitude higher for microgel-containing adhesive when compared to those for microgel-free sample. This observation indicated that the catechol likely reacted quickly with nucleophilic groups (i.e., $-NH_2$ of lysine) found on the surface of the microgel and that the microgel-incorporated adhesives can potentially dissipate fracture energy immediately after curing.

Lap Shear Adhesion Testing. The lap shear strength increased with the incorporation of gelatin microgel (Figure 6).

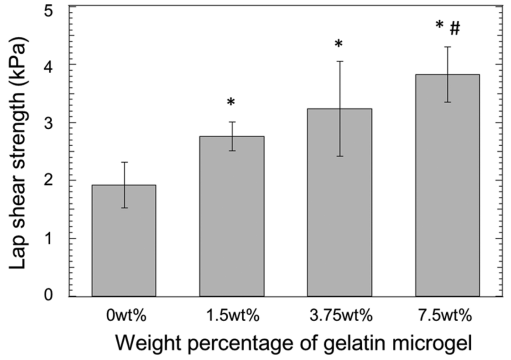

Figure 6. Lap shear adhesion test results of PEGDM adhesive with different weight percentage of gelatin microgel: (∗) $p < 0.05$ when compared to adhesive containing 0 wt % microgel; (#) $p < 0.05$ when compared to adhesive containing 1.5 wt % microgel. Error bars indicate the standard deviation, and $n = 5$.

Measured values for gelatin containing formulations were significantly higher (1.5- to 2-fold) when compared to microgel-free control. This increase in the adhesive property is attributed to the increased mechanical properties of the microgel-containing adhesive. This observation is consistent with previously published reports where increased bulk cohesive properties of an adhesive greatly enhanced its adhesive properties.[25,40,41] The lap shear strength values reported here are lower compared to values reported for other catechol-modified PEG adhesives (10−40 kPa).[42−44] However, it is difficult to compare these results directly due to the usage of different tissue substrates and testing protocols between these studies (i.e., different methods used to prepare samples, strain rate, etc.).

In Vitro Degradation. In the in vitro degradation test (Figure 7), adhesives with different weight percentage of gelatin

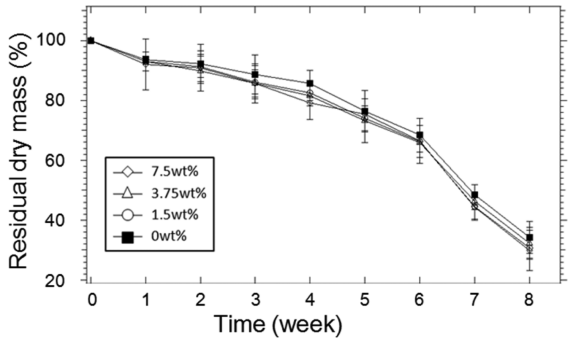

Figure 7. In vitro degradation of PEGDM adhesives containing different weight percentages of gelatin microgel. Error bars indicate the standard deviation, and $n = 3$.

microgel degraded at a similar rate. Regardless of the formulation, the adhesives lost over 70% of their dry mass over an 8-week period. After which point, all the adhesive samples were completely degraded. There was no significant difference between the formulations, indicating that degradation occurred mainly through the hydrolysis of the ester bond between the PEG and glutaric acid. The degradation behavior of PEGDM adhesive is comparable to PEG-based adhesive containing similar PEG-glutaric acid linkage.[25,45]

Cell Viability Assessment. The incorporation of gelatin microgel did not affect the cytocompatibility of PEGDM adhesive (Figure 8). All the formulations tested exhibited

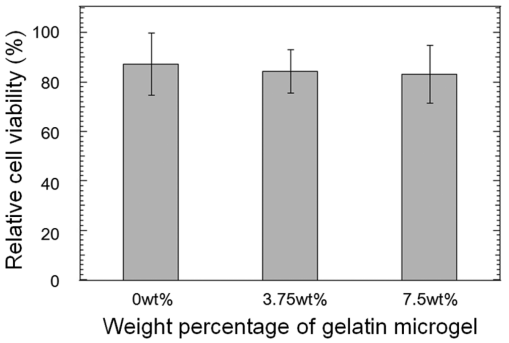

Figure 8. Relative cell viability for L929 fibroblast exposed to PEGDM adhesives containing different weight percentages of gelatin microgel. Error bars indicate the standard deviation, and $n = 9$.

relative cell viability greater than 82%. Gelatin has a track record of being a biocompatible biomaterial.[7−9,13] Additionally, various catechol-modified PEG hydrogels were reported to be biocompatible.[24,25,43,44] As expected, the composite adhesive composed of gelatin and PEGDM was noncytotoxic.

Cell Attachment Assay. Primary rat dermal fibroblasts were seeded onto the surface of PEGDM adhesive and the cellular density of the attached cells was quantified after DAPI staining (Figure S4). The cell number increased significantly with increasing weight percentage of gelatin microgel (Figure 9). The number of attached cells on the surface of adhesive

DOI: 10.1021/acsami.6b01364
ACS Appl. Mater. Interfaces 2016, 8, 11980−11989

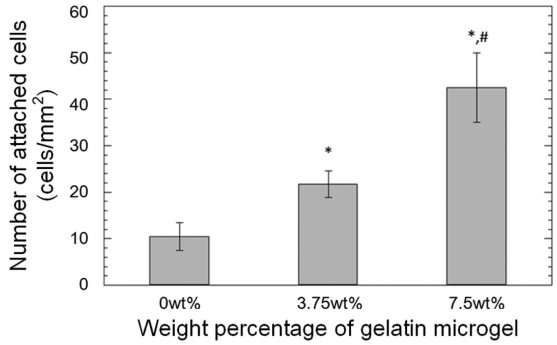

Figure 9. Number of attached rat dermal fibroblasts on the surface of the adhesive based on DAPI staining: (∗) $p < 0.05$ when compared to adhesive containing 0 wt % microgel; (#) $p < 0.05$ when compared to adhesive containing 3.75 wt % microgel. Error bars indicate the standard deviation, and $n = 3$.

containing 7.5 wt % microgel was about 4 times higher when compared to that of the microgel-free control. Calcine and ethidium bromide were used to stain living (green) and dead (red) cells, respectively, attached to the surface of the adhesive (Figure 10). For the microgel-free PEGDM adhesive (Figure 10A), there were 3 times as many dead cells as there were living cells and the attached living cells appeared rounded in shape, which is an indication of poor attachment.[26] On the other hand, most of the cells that were attached to the surface of microgel-containing PEGDM appeared to be well spread in morphology (Figure 10B and Figure 10C). Most importantly, no dead cells were found on the surface of these adhesives. Gelatin microgels were also stained green through nonspecific binding (blue arrows in Figure 10B and Figure 10C), and there is evidence for colocalization of the attached cells and the underlying gelatin microgels. Similar observations were noted for images stained with DAPI (Figure S4) to support the colocalization of attached cells and gelatin microgels. The presence of gelatin provides binding sites for the fibroblast to attach on and the successful attachment is critical for the survival and proliferation for these cells.[8,46−48]

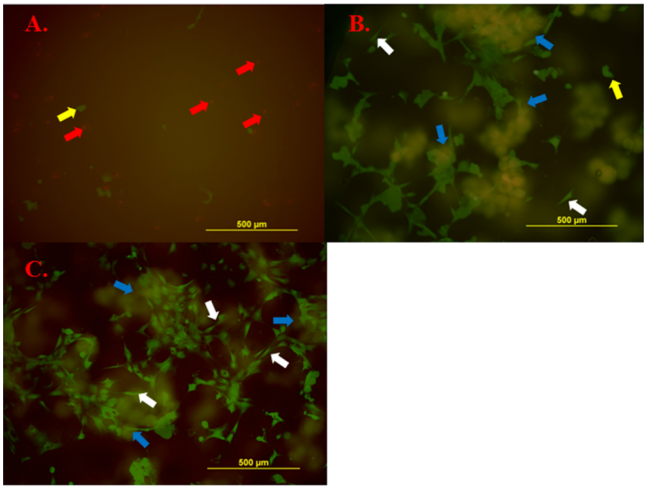

Figure 10. Live/dead staining of rat dermal fibroblasts attached to the surface of PEGDM containing 0 (A), 3.75 (B), and 7.5 wt % (C) of gelatin microgel. Living cells were stained in green, and dead cells were stained in red. Gelatin microgels also appeared in green through nonspecific binding. Blue arrow: gelatin microgel. White arrow: spread cells. Red arrow: dead cells. Yellow arrow: living cells but not spread.

Subcutaneous Implantation. PEGDM adhesives containing 0 and 7.5 wt % gelatin microgel were subcutaneously implanted into rats for 2 and 6 weeks to evaluate the in vivo biocompatibility and bioactivity of the adhesives. Trichrome staining revealed that after 2 weeks of implantation, more cells were present near the tissue-adhesive interface for the microgel containing adhesive (7.7 ± 0.90 cells/mm^2) when compared to that of the microgel-free adhesive (5.3 ± 0.8 cells/mm^2) (Table 2 and Figure 11A and Figure 11B). From immunofluorescent staining of both adhesive formulations, M1 macrophages and fibroblast were observed near the tissue-adhesive interface (Figure 11C,D,G,H), while M2 cells were found further away from interface (Figure 11E,F). After 6 weeks of implantation, a higher cell density was also found at the tissue-adhesive interface for the microgel-containing adhesive (3.4 ± 0.64 cells/mm^2) when compared to the microgel-free PEGDM (2.02 ± 0.66 cells/mm^2) (Figure 12A,B). However, when compared to the result of 2 weeks test, there was a decrease in cell density at the 6-week time point (Table 2). The thickness of collagen deposition around 7.5 wt % adhesive (74.3 ± 14.1 μm) was also higher than that surrounding the 0 wt % adhesive (43.6 ± 14.4 μm) (Figure 12A,B). Fibroblast and macrophage were observed in the same area as the result of 2 weeks implantation (Figure 12C−H).

Results from the implantation study indicated that PEGDM adhesive and its composite are biocompatible. Both formulations exhibited typical acute inflammatory response and the reduction in cell density after 6 weeks of implantation indicating a reduced inflammatory response over time.[49] The deposition of collagen and the existence of M2 macrophage are signs of wound healing.[50−54] The microgel-containing adhesive recruited higher number of cells to its interface as a result macrophage activation by gelatin.[55,56] Subsequently, more fibroblasts were recruited and resulted in elevated deposition of collagen matrix.[57] The higher amount of collagen deposition indicates that the composite adhesive is likely not suitable for repairing tissues rich in vasculatures, as it may hinder the molecular exchange between implanted materials and surrounding tissues.[58] However, the adhesive may potentially be suitable for the repair connective tissues.

One unique observation for adhesive containing gelatin microgel is the presence of a pocket of cellular infiltration at the

Table 2. Cell Density, Cell Infiltration Layer, and Collagen Layer Thickness after 2 and 6 Weeks Subcutaneous Implantation[a]

	2 weeks		6 weeks	
	0 wt %	7.5 wt %	0 wt %	7.5 wt %
cell density in tissue-adhesive interface (×10^3 cells/mm^2)	5.3 ± 0.80	7.7 ± 0.90*	2.0 ± 0.66	3.4 ± 0.64*
cell infiltration layer (μm)			95.8 ± 14.4	97.2 ± 16.8
collagen layer thickness (μm)			43.6 ± 14.5	74.3 ± 14.1*

[a]The symbol indicates the following: (∗) $p < 0.05$ when compared to 0 wt % adhesive.

DOI: 10.1021/acsami.6b01364
ACS Appl. Mater. Interfaces 2016, 8, 11980−11989

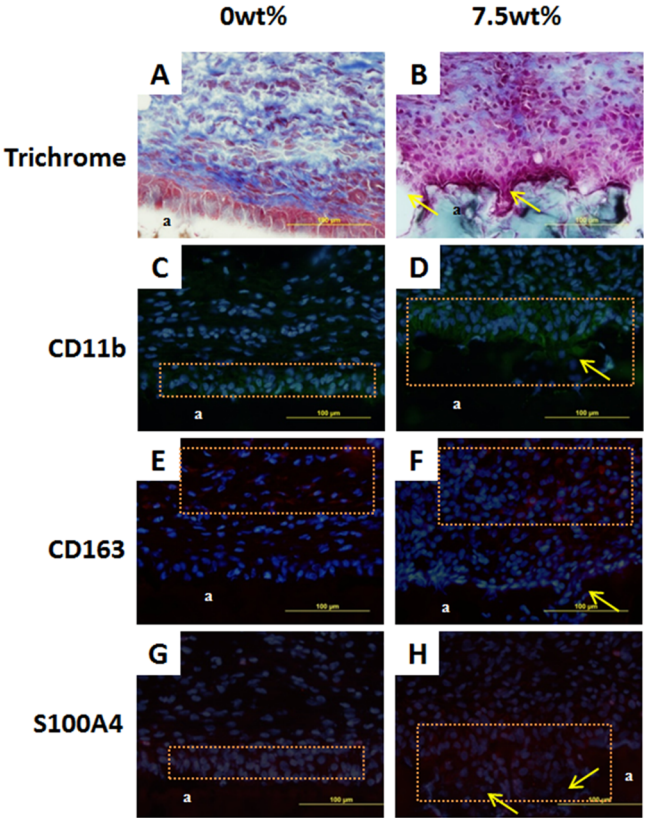

Figure 11. Masson's trichrome stain (A, B) and immunofluorescent stain (C–H) of 0 and 7.5 wt % adhesive and surrounding tissue after 2 weeks subcutaneous implantation. a: adhesive. Orange box: cell distribution area. Single headed arrow: cell infiltrating into the pocket formed via gelatin microgel degradation. Blue (DAPI): cell nuclei. Green (CD11b): macrophage. Red (CD163 and S100A4): M2 macrophage and fibroblast, respectively.

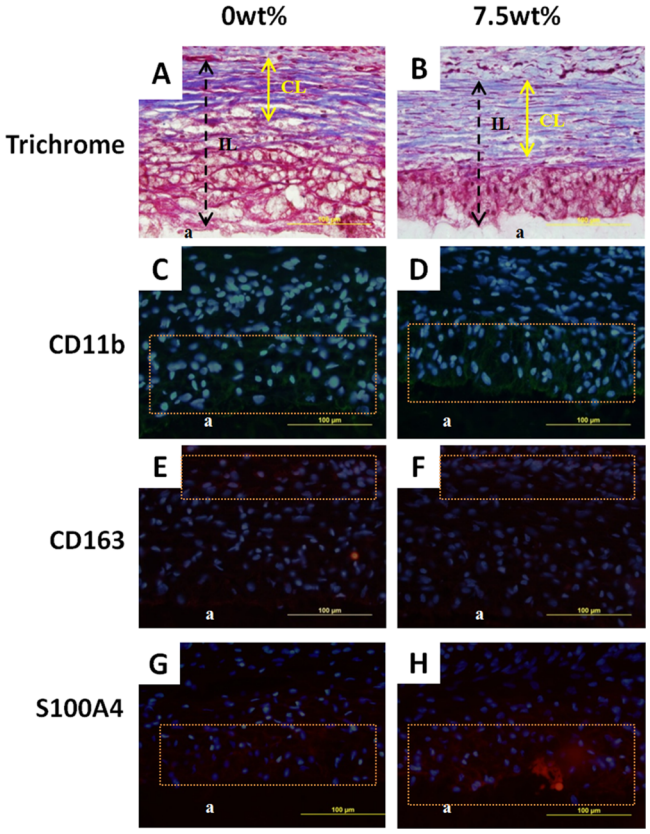

Figure 12. Masson's trichrome stain (A, B) and immunofluorescent stain (C–H) of 0 and 7.5 wt % adhesive and surrounding tissue after 6 weeks subcutaneous implantation. a: adhesive. Orange box: cell distribution area. Double headed arrow: collagen layer (CL in A and B). Dashed arrow: cell infiltration layer (IL in A and B). Blue (DAPI): cell nuclei. Green (CD11b): macrophage. Red (CD163 and S100A4): M2 macrophage and fibroblast, respectively.

interface of the adhesive that previously contained a microgel (single headed arrows in Figure 11). The pocket of cellular infiltration was clearly visible and rounded in shape after 2 weeks of implantation but became less defined at the later time point, potentially due to the degradation of surrounding PEGDM adhesive. On the other hand, no cell infiltration was observed for microgel-free PEGDM adhesive. Gelatin microgels were readily degraded by the invading cells and provided space for cell infiltration. We had previously incorporated biodegradable nanosilicate, laponite, to enhance the bioactivity of PEG-based adhesive.[25] However, due to the small size of these nanoparticles (30 nm diameter and 1 nm thick discs) relative to a mammalian cell (~10 μm), in vivo cellular infiltration was not observed until 8 weeks postimplantation. On the other hand, gelatin microgels used in the present study are larger in size (i.e., ~50 μm) when compared to that of an invading cell, and this size difference contributed to rapid cellular infiltration. However, the PEG matrix acted as a barrier for the continued advancement of these cells, as there was no significant difference on the average infiltration layer (IL) thickness between the two formulations after 6 weeks of implantation (Table 2). This also indicated that the adhesives degraded predominantly through hydrolysis of the ester linkage between PEG and glutaric acid. Gelatin microgel incorporation demonstrated to be a useful strategy to promote cell infiltration which is necessary for rapid tissue integration. However, both the concentrations of PEGDM and gelatin microgel need to be further tuned to allow cellular infiltration to occur rapidly across the bulk of the adhesive network.

CONCLUSION

Incorporation of gelatin microgel was demonstrated to simultaneously improve the adhesive properties and the bioactivity of PEGDM adhesive. Increasing microgel content increased the bulk mechanical properties of the adhesive matrix without sacrificing its compliance, due to the presence of physical bonds found within the gelatin microgels. Elevated bulk mechanical properties improved the adhesive properties of the composite adhesive. Additionally, gelatin microgels provided binding sites for cellular attachment in culture and were readily degraded in vivo to provide space for rapid cell infiltration. However, the PEGDM matrix acted as a barrier for continued cell infiltration and the composition of the adhesive needs to be further tuned to improve the rate of cell infiltration across the bulk of the adhesive.

ASSOCIATED CONTENT

Supporting Information

The Supporting Information is available free of charge on the ACS Publications website at DOI: 10.1021/acsami.6b01364.

NMR spectra of PEGGlu and PEGDM, SEM image of gelatin microgel, and DAPI staining of rat dermal fibroblasts for cell attachment test (PDF)

DOI: 10.1021/acsami.6b01364
ACS Appl. Mater. Interfaces 2016, 8, 11980–11989

AUTHOR INFORMATION

Corresponding Author

*E-mail: bplee@mtu.edu. Phone: (906) 487-3262.

Notes

The authors declare no competing financial interest.

ACKNOWLEDGMENTS

This project was supported by the National Institutes of Health under the Award R15GM104846. Yuting Li was supported in part by Kenneth L. Stevenson Biomedical Engineering Summer Research Fellowship.

REFERENCES

(1) Lin, C. C.; Anseth, K. S. PEG Hydrogels for the Controlled Release of Biomolecules in Regenerative Medicine. *Pharm. Res.* **2009**, *26*, 631−643.
(2) Graham, N. B. Poly(ethylene oxide) and Related Hydrogels. In *Hydrogels in Medicine and Pharmacy*; Peppas, N. A., Ed.; CRC Press Inc.: Boca Raton, FL, 1987; Vol. 2, pp 95−113.
(3) Shin, H.; Ruhe, P. Q.; Mikos, A. G.; Jansen, J. A. In Vivo Bone and Soft Tissue Response to Injectable, Biodegradable Oligo (Poly (Ethylene Glycol) Fumarate) Hydrogels. *Biomaterials* **2003**, *24*, 3201−3211.
(4) Shin, H.; Jo, S.; Mikos, A. G. Modulation of Marrow Stromal Osteoblast Adhesion on Biomimetic Oligo [Poly (Ethylene Glycol) Fumarate] Hydrogels Modified with Arg-Gly-Asp Peptides and a Poly (Ethylene Glycol) Spacer. *J. Biomed. Mater. Res.* **2002**, *61*, 169−179.
(5) Hubbell, J. A.; Massia, S. P.; Desai, N. P.; Drumheller, P. D. Endothelial Cell-Selective Materials for Tissue Engineering in the Vascular Graft Via a New Receptor. *Bio/Technology* **1991**, *9*, 568−572.
(6) Chung, I.-M.; Enemchukwu, N. O.; Khaja, S. D.; Murthy, N.; Mantalaris, A.; García, A. J. Bioadhesive Hydrogel Microenvironments to Modulate Epithelial Morphogenesis. *Biomaterials* **2008**, *29*, 2637−2645.
(7) te Nijenhuis, K. *Gelatin*; Springer: Berlin, 1997.
(8) Rosellini, E.; Cristallini, C.; Barbani, N.; Vozzi, G.; Giusti, P. Preparation and Characterization of Alginate/Gelatin Blend Films for Cardiac Tissue Engineering. *J. Biomed. Mater. Res., Part A* **2009**, *91*, 447−453.
(9) Bigi, A.; Cojazzi, G.; Panzavolta, S.; Rubini, K.; Roveri, N. Mechanical and Thermal Properties of Gelatin Films at Different Degrees of Glutaraldehyde Crosslinking. *Biomaterials* **2001**, *22*, 763−768.
(10) Sung, H. W.; Huang, D. M.; Chang, W. H.; Huang, R. N.; Hsu, J. C. Evaluation of Gelatin Hydrogel Crosslinked with Various Crosslinking Agents as Bioadhesives: In Vitro Study. *J. Biomed. Mater. Res.* **1999**, *46*, 520−530.
(11) Chvapil, M. Collagen Sponge: Theory and Practice of Medical Applications. *J. Biomed. Mater. Res.* **1977**, *11*, 721−741.
(12) Sela, M.; Arnon, R. Studies on the Chemical Basis of the Antigenicity of Proteins. 1. Antigenicity of Polypeptidyl Gelatins. *Biochem. J.* **1960**, *75*, 91.
(13) Vandelli, M.; Rivasi, F.; Guerra, P.; Forni, F.; Arletti, R. Gelatin Microspheres Crosslinked with D, L-Glyceraldehyde as a Potential Drug Delivery System: Preparation, Characterisation, in Vitro and in Vivo Studies. *Int. J. Pharm.* **2001**, *215*, 175−184.
(14) Kawai, K.; Suzuki, S.; Tabata, Y.; Ikada, Y.; Nishimura, Y. Accelerated Tissue Regeneration through Incorporation of Basic Fibroblast Growth Factor-Impregnated Gelatin Microspheres into Artificial Dermis. *Biomaterials* **2000**, *21*, 489−499.
(15) Lee, B. P.; Messersmith, P. B.; Israelachvili, J. N.; Waite, J. H. Mussel-Inspired Adhesives and Coatings. *Annu. Rev. Mater. Res.* **2011**, *41*, 99−132.
(16) Waite, J. H. Nature's Underwater Adhesive Specialist. *Int. J. Adhes. Adhes.* **1987**, *7*, 9−14.
(17) Lee, B. P.; Dalsin, J. L.; Messersmith, P. B. Synthesis and Gelation of Dopa-Modified Poly(Ethylene Glycol) Hydrogels. *Biomacromolecules* **2002**, *3*, 1038−1047.
(18) Lee, H.; Scherer, N. F.; Messersmith, P. B. Single Molecule Mechanics of Mussel Adhesion. *Proc. Natl. Acad. Sci. U. S. A.* **2006**, *103*, 12999−13003.
(19) Sugumaran, M.; Dali, H.; Semensi, V. Chemical- and Cuticular Phenoloxidase-Mediated Synthesis of Cysteinyl-Catechol Adducts. *Arch. Insect Biochem. Physiol.* **1989**, *11*, 127−137.
(20) Moulay, S. Dopa/Catechol-Tethered Polymers: Bioadhesives and Biomimetic Adhesive Materials. *Polym. Rev.* **2014**, *54*, 436−513.
(21) Laulicht, B.; Mancini, A.; Geman, N.; Cho, D.; Estrellas, K.; Furtado, S.; Hopson, R.; Tripathi, A.; Mathiowitz, E. Bioinspired Bioadhesive Polymers: Dopa-Modified Poly (Acrylic Acid) Derivatives. *Macromol. Biosci.* **2012**, *12*, 1555−1565.
(22) Meng, H.; Li, Y.; Faust, M.; Konst, S.; Lee, B. P. Hydrogen Peroxide Generation and Biocompatibility of Hydrogel-Bound Mussel Adhesive Moiety. *Acta Biomater.* **2015**, *17*, 160−169.
(23) Cencer, M.; Murley, M.; Liu, Y.; Lee, B. P. Effect of Nitro-Functionalization on the Cross-Linking and Bioadhesion of Biomimetic Adhesive Moiety. *Biomacromolecules* **2015**, *16*, 404−410.
(24) Cencer, M. M.; Liu, Y.; Winter, A.; Murley, M.; Meng, H.; Lee, B. P. Effect of Ph on the Rate of Curing and Bioadhesive Properties of Dopamine Functionalized Poly(Ethylene Glycol) Hydrogels. *Biomacromolecules* **2014**, *15*, 2861−2869.
(25) Liu, Y.; Meng, H.; Konst, S.; Sarmiento, R.; Rajachar, R.; Lee, B. P. Injectable Dopamine-Modified Poly(Ethylene Glycol) Nanocomposite Hydrogel with Enhanced Adhesive Property and Bioactivity. *ACS Appl. Mater. Interfaces* **2014**, *6*, 16982−16992.
(26) Yun, E. J.; Yon, B.; Joo, M. K.; Jeong, B. Cell Therapy for Skin Wound Using Fibroblast Encapsulated Poly (Ethylene Glycol)-Poly (L-Alanine) Thermogel. *Biomacromolecules* **2012**, *13*, 1106−1111.
(27) Kuijpers, A.; Engbers, G.; Feijen, J.; De Smedt, S.; Meyvis, T.; Demeester, J.; Krijgsveld, J.; Zaat, S.; Dankert, J. Characterization of the Network Structure of Carbodiimide Cross-Linked Gelatin Gels. *Macromolecules* **1999**, *32*, 3325−3333.
(28) Kuijpers, A.; Van Wachem, P.; Van Luyn, M.; Plantinga, J.; Engbers, G.; Krijgsveld, J.; Zaat, S.; Dankert, J.; Feijen, J. In Vivo Compatibility and Degradation of Crosslinked Gelatin Gels Incorporated in Knitted Dacron. *J. Biomed. Mater. Res.* **2000**, *51*, 136−145.
(29) Anseth, K. S.; Bowman, C. N.; Brannon-Peppas, L. Mechanical Properties of Hydrogels and Their Experimental Determination. *Biomaterials* **1996**, *17*, 1647−1657.
(30) Mulder, M.; Crosier, J.; Dunn, R. Cauda Equina Compression by Hydrogel Dural Sealant after a Laminotomy and Discectomy Case Report. *Spine* **2009**, *34*, E144−E148.
(31) Blackburn, S. L.; Smyth, M. D. Hydrogel-Induced Cervicomedullary Compression after Posterior Fossa Decompression for Chiari Malformation - Case Report. *J. Neurosurg.* **2007**, *106*, 302−304.
(32) Ding, X.; Vegesna, G. K.; Meng, H.; Winter, A.; Lee, B. P. Nitro-Group Functionalization of Dopamine and Its Contribution to the Viscoelastic Properties of Catechol-Containing Nanocomposite Hydrogels. *Macromol. Chem. Phys.* **2015**, *216*, 1109−1119.
(33) Lee, B. P.; Lin, M.-H.; Narkar, A.; Konst, S.; Wilharm, R. Modulating the Movement of Hydrogel Actuator Based on Catechol-Iron Ion Coordination Chemistry. *Sens. Actuators, B* **2015**, *206*, 456−462.
(34) Moura, M. J.; Figueiredo, M. M.; Gil, M. H. Rheological Study of Genipin Cross-Linked Chitosan Hydrogels. *Biomacromolecules* **2007**, *8*, 3823−3829.
(35) Liu, M.; Li, W.; Rong, J.; Zhou, C. Novel Polymer Nanocomposite Hydrogel with Natural Clay Nanotubes. *Colloid Polym. Sci.* **2012**, *290*, 895−905.
(36) Skelton, S.; Bostwick, M.; O'Connor, K.; Konst, S.; Casey, S.; Lee, B. P. Biomimetic Adhesive Containing Nanocomposite Hydrogel with Enhanced Materials Properties. *Soft Matter* **2013**, *9*, 3825−3833.

DOI: 10.1021/acsami.6b01364
ACS Appl. Mater. Interfaces 2016, 8, 11980−11989

(37) Djabourov, M.; Papon, P. Influence of Thermal Treatments on the Structure and Stability of Gelatin Gels. *Polymer* **1983**, *24*, 537−542.
(38) de Carvalho, W.; Djabourov, M. Physical Gelation under Shear for Gelatin Gels. *Rheol. Acta* **1997**, *36*, 591−609.
(39) Byun, E.; Ryu, J. H.; Lee, H. Catalyst-mediated yet catalyst-free hydrogels formed by interfacial chemical activation. *Chem. Commun.* **2014**, *50*, 2869−2872.
(40) da Silva, L. F. M.; Rodrigues, T. N. S. S.; Figueiredo, M. A. V.; de Moura, M. F. S. F.; Chousal, J. A. G. Effect of Adhesive Type and Thickness on the Lap Shear Strength. *J. Adhes.* **2006**, *82*, 1091−1115.
(41) Murphy, J. L.; Vollenweider, L.; Xu, F.; Lee, B. P. Adhesive Performance of Biomimetic Adhesive-Coated Biologic Scaffolds. *Biomacromolecules* **2010**, *11*, 2976−2984.
(42) Burke, S. A.; Ritter-Jones, M.; Lee, B. P.; Messersmith, P. B. Thermal Gelation and Tissue Adhesion of Biomimetic Hydrogels. *Biomed. Mater.* **2007**, *2*, 203−210.
(43) Mehdizadeh, M.; Weng, H.; Gyawali, D.; Tang, L.; Yang, J. Injectable Citrate-Based Mussel-Inspired Tissue Bioadhesives with High Wet Strength for Sutureless Wound Closure. *Biomaterials* **2012**, *33*, 7972−7983.
(44) Brubaker, C. E.; Messersmith, P. B. Enzymatically Degradable Mussel-Inspired Adhesive Hydrogel. *Biomacromolecules* **2011**, *12*, 4326−4334.
(45) Lin, M.-H.; Anderson, J.; Pinnaratip, R.; Meng, H.; Konst, S.; DeRouin, A. J.; Rajachar, R.; Ong, K. G.; Lee, B. P. Monitoring the Long-Term Degradation Behavior of Biomimetic Bioadhesive Using Wireless Magnetoelastic Sensor. *IEEE Trans. Biomed. Eng.* **2015**, *62*, 1838−1842.
(46) Tabata, Y.; Ikada, Y. Protein Release from Gelatin Matrices. *Adv. Drug Delivery Rev.* **1998**, *31*, 287−301.
(47) Heris, H. K.; Rahmat, M.; Mongeau, L. Characterization of a Hierarchical Network of Hyaluronic Acid/Gelatin Composite for Use as a Smart Injectable Biomaterial. *Macromol. Biosci.* **2012**, *12*, 202−210.
(48) Wu, S.-C.; Chang, W.-H.; Dong, G.-C.; Chen, K.-Y.; Chen, Y.-S.; Yao, C.-H. Cell Adhesion and Proliferation Enhancement by Gelatin Nanofiber Scaffolds. *J. Bioact. Compat. Polym.* **2011**, *26*, 565−577.
(49) Anderson, J. M.; Shive, M. S. Biodegradation and Biocompatibility of Pla and Plga Microspheres. *Adv. Drug Delivery Rev.* **2012**, *64*, 72−82.
(50) Velnar, T.; Bailey, T.; Smrkolj, V. The Wound Healing Process: An Overview of the Cellular and Molecular Mechanisms. *J. Int. Med. Res.* **2009**, *37*, 1528−1542.
(51) Badylak, S. F.; Valentin, J. E.; Ravindra, A. K.; McCabe, G. P.; Stewart-Akers, A. M. Macrophage Phenotype as a Determinant of Biologic Scaffold Remodeling. *Tissue Eng., Part A* **2008**, *14*, 1835−1842.
(52) Guo, S.; DiPietro, L. A. Factors Affecting Wound Healing. *J. Dent. Res.* **2010**, *89*, 219−229.
(53) Gosain, A.; DiPietro, L. A. Aging and Wound Healing. *World J. Surg.* **2004**, *28*, 321−326.
(54) Anderson, J. M.; Rodriguez, A.; Chang, D. T. Foreign Body Reaction to Biomaterials. *Semin. Immunol.* **2008**, *20*, 86−100.
(55) Anderson, J. M.; Miller, K. M. Biomaterial Biocompatibility and the Macrophage. *Biomaterials* **1984**, *5*, 5−10.
(56) Tabata, Y.; Ikada, Y. Macrophage Activation through Phagocytosis of Muramyl Dipeptide Encapsulated in Gelatin Microspheres. *J. Pharm. Pharmacol.* **1987**, *39*, 698−704.
(57) Diegelmann, R. F.; Evans, M. C. Wound Healing: An Overview of Acute, Fibrotic and Delayed Healing. *Front. Biosci., Landmark Ed.* **2004**, *9*, 283−289.
(58) Ravin, A. G.; Olbrich, K. C.; Levin, L. S.; Usala, A. L.; Klitzman, B. Long- and Short-Term Effects of Biological Hydrogels on Capsule Microvascular Density around Implants in Rats. *J. Biomed. Mater. Res.* **2001**, *58*, 313−318.

DOI: 10.1021/acsami.6b01364
ACS Appl. Mater. Interfaces 2016, 8, 11980−11989